© 2014. Published by The Company of Biologists Ltd | Development (2014) 141, 4817-4826 doi:10.1242/dev.113415

RESEARCH ARTICLE

Programmed cell cycle arrest is required for infection of corn plants by the fungus *Ustilago maydis*

Sónia Castanheira, Natalia Mielnichuk and José Pérez-Martín*

ABSTRACT

Ustilago maydis is a plant pathogen that requires a specific structure called infective filament to penetrate the plant tissue. Although able to grow, this filament is cell cycle arrested on the plant surface. This cell cycle arrest is released once the filament penetrates the plant tissue. The reasons and mechanisms for this cell cycle arrest are unknown. Here, we have tried to address these questions. We reached three conclusions from our studies. First, the observed cell cycle arrest is the result of the cooperation of at least two distinct mechanisms: one involving the activation of the DNA damage response (DDR) cascade; and the other relying on the transcriptional downregulation of Hsl1, a kinase that modulates the G2/M transition. Second, a sustained cell cycle arrest during the infective filament step is necessary for the virulence in *U. maydis*, as a strain unable to arrest the cell cycle was severely impaired in its ability to infect corn plants. Third, production of the appressorium, a structure required for plant penetration, is incompatible with an active cell cycle. The inability to infect plants by strains defective in cell cycle arrest seems to be caused by their failure to induce the appressorium formation process. In summary, our findings uncover genetic circuits to arrest the cell cycle during the growth of this fungus on the plant surface, thus allowing the penetration into plant tissue.

KEY WORDS: Appressorium, Cell cycle, *Ustilago maydis*, Virulence

INTRODUCTION

Pathogenic fungi are characterized by a great diversity in their lifestyles and, as a consequence, in the symptoms they cause. This is an important caveat for the search of common targets in antifungal research, as different attributes might be important for each fungus to cause disease. However, despite such diversity, all of them share the requirement of accurate developmental decisions for the induction of the virulence program. Developmental decisions often involve differentiation processes that need the reset of the cell cycle and the induction of a new morphogenetic program. Therefore, the understanding of how growth and cell cycle progression are regulated coordinately during pathogenic development seems to be an alternative way to cope with fungal infections. Although efforts have been made for various fungal systems, there is still limited information available regarding the relationship of these processes with the induction of the virulence programs (Sudbery and Gladfelter, 2008). Hence, the role of fungal cell cycle regulators – which are widely conserved elements – as true virulence factors has yet to be defined.

Instituto de Biología Funcional y Genómica, Consejo Superior de Investigaciones Científicas, Zacarías González 2, Salamanca 37007, Spain.

*Author for correspondence (jose.perez@csic.es)

Received 27 May 2014; Accepted 24 October 2014

The corn smut fungus *Ustilago maydis* represents an excellent model to study the relationships between cell cycle, morphogenesis and pathogenicity (Perez-Martin et al., 2006; Steinberg and Perez-Martin, 2008). The activation of the virulence program in *U. maydis* involves the mating of a pair of compatible haploid budding cells to produce an infectious dikaryotic hypha. This process implies strong morphological changes (bud-to-hypha transition) as well as genetic changes (haploid-to-dikaryotic transition), advocating for an accurate control of the cell cycle and morphogenesis during these transitions (Perez-Martin, 2012). For example, the formation of the infective filament in *U. maydis*, which is the first step in the pathogenic process, relies on a dual process that involves a specific G2 cell cycle arrest as well as the activation of strong polar growth (Perez-Martin and Castillo-Lluva, 2008). On the plant surface, this cell cycle-arrested hypha expands by apical growth, with the cytoplasm accumulating at the tip cell compartment. The older parts of the hypha become vacuolated and are sealed off by insertion of regularly spaced septa at the distal pole. This results in the formation of characteristic empty sections, which often collapse (Steinberg et al., 1998). Eventually, the hypha stops polar growth in response to unidentified plant signals and forms the appressorium, a structure that adheres to the plant surface to achieve penetration (Snetselaar and Mims, 1993). Appressorium formation is mandatory for the infection to proceed, as *U. maydis* mutant strains unable to produce functional appressoria are avirulent (Berndt et al., 2010; Fernandez-Alvarez et al., 2009; Freitag et al., 2011; Lanver et al., 2010). Once the filament enters the plant, the cell cycle is reactivated. The formation of empty sections ceases and mitotic divisions take place, concomitant with the development of clamp-like structures that allow the correct sorting of nuclei to maintain the dikaryotic status (de Sena-Tomas et al., 2011; Scherer et al., 2006). In this way the fungus proliferates within the plant, inducing the formation of tumors, in which diploid teliospores are eventually generated.

A peculiar characteristic of the *U. maydis* dikaryotic infective filament is the sustained cell cycle arrest at G2 phase while growing on the plant surface. However, it seems to be a more general feature, as this arrest has also been described in rust fungi, such as *Uromyces phaseoli* (Heath and Heath, 1979). The biological function of the cell cycle arrest is not known. One possibility is that the suppression of the M phase enables the fungus to explore efficiently the host surface, as tip growth occurs in G2 phase only (Perez-Martin and Castillo-Lluva, 2008). Alternatively, tight cell cycle control could be linked to the developmental program as such, as described in metazoans (Budirahardja and Gonczy, 2009). To further understand the role of the cell cycle control in pathogenicity, we aimed to uncouple the cell cycle arrest from other developmental processes during early invasive growth.

Previous research from our group has shown that efficient cell cycle arrest during the infective filament formation requires the cooperation of elements from the DNA damage response (DDR) cascade, such as the kinase Chk1 and its upstream activating kinase

Development (2014) 141, 4817-4826 doi:10.1242/dev.113415

Atr1 (de Sena-Tomas et al., 2011; Mielnichuk et al., 2009; Perez-Martin, 2009). During the early stages of formation of the infective hypha, the Chk1 kinase is activated for a short period of time, resulting in a transient G2 cell cycle arrest (Mielnichuk et al., 2009). Our current hypothesis is that the activation of the DDR cascade provides a time frame during which additional mechanisms are recruited to sustain a long-term cell cycle arrest. The nature of these proposed additional elements is unknown. Our results indicate that transcriptional downregulation of a Nim1-like kinase, Hsl1, cooperates together with the Chk1 transient activation to produce a permanent cell cycle arrest at G2 phase. We have disabled this cell cycle arrest during the infection process and have found that the absence of this cell cycle arrest renders cells unable to infect the plant. Finally, we have traced the virulence defect to the inability to produce appressoria.

RESULTS

Induction of *b* gene expression results in downregulation of the gene encoding the Nim1-like kinase Hsl1

The formation of the infectious hypha in *U. maydis* depends on an intricate transcriptional program that primarily involves the master transcriptional regulator b-factor (Feldbrugge et al., 2004). Production of this regulator is linked to the mating process that, after cell fusion, leads to the interaction of the two subunits (bW and bE) composing the b-factor, each subunit being provided by each mating partner. Our rationale was that the additional elements required for sustained cell cycle arrest during the formation of the infective filament might be cell cycle regulatory genes, the transcriptional levels of which might be affected by the b-dependent transcriptional program. In fact, previous studies analyzing the *U. maydis* transcriptome found that mRNA levels of several cell cycle regulatory genes decreased upon *b*-expression (Heimel et al., 2010). However, caution should be exercised when analyzing the expression of cell cycle genes because the transcription of cell cycle genes is linked to an active cell cycle. Thus, downregulation of these genes could be merely a consequence of the b-induced cell cycle arrest. Therefore, it would be difficult to conclude whether the decrease in the levels of these regulators is a cause or a consequence of the cell cycle arrest.

To address this dilemma, we have analyzed the expression of genes encoding G2/M regulators in conditions of *b*-expression and non-arrested cell cycle. To achieve this, we took advantage of a *U. maydis* strain that expresses simultaneously the genes encoding the b-factor as well as an ectopic Cdk1 allele refractory to inhibitory phosphorylation at Tyr15 (*cdk1*^{AF}), the ultimate cause of the b-induced G2 cell cycle arrest (Mielnichuk et al., 2009; Sgarlata and Perez-Martin, 2005b). In this strain, despite the activation of the b-dependent transcriptional program, the cell cycle is not arrested (Mielnichuk et al., 2009) (Fig. 1A). To express the b-factor, we used the haploid *U. maydis* strains AB33 and AB34 that harbor the compatible *bE1* and *bW2* and non-compatible *bE1* and *bW1* genes, respectively, both under the control of the nitrate-inducible *nar1* promoter (Brachmann et al., 2001). Induction of *bE1/bW2* in the compatible strain AB33 growing in medium with nitrate results in a filament that resembles the infectious hypha formed after fusion of compatible haploid cells. The *cdk1* alleles [mutant and wild type (WT) as a control] were also expressed under the *nar1* promoter, to induce both classes of genes (the b-factor-encoding genes and *cdk1* alleles) simultaneously.

We included in our transcription analysis well-characterized *U. maydis* G2/M regulatory genes, such as the B-cyclins *clb1* and *clb2* (Garcia-Muse et al., 2004), the *wee1* kinase (Sgarlata and Perez-Martin, 2005b) and the *cdc25* phosphatase (Sgarlata and Perez-Martin, 2005a). We also included genes putatively encoding G2/M regulators, the transcriptional levels of which were shown to be altered upon *b*-expression in a recent genome-wide transcriptomic analysis (Heimel et al., 2010). These regulators included *um03234.2*, encoding a homolog to the Polo kinase and renamed Plk1, and *um03928*, encoding a Nim1-like kinase and renamed Hsl1.

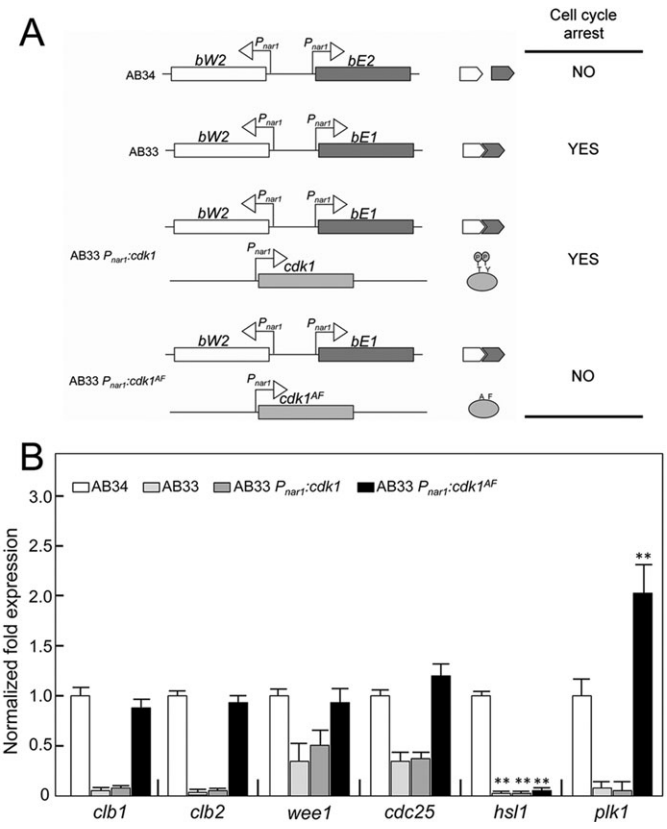

Fig. 1. Transcriptional downregulation of *hsl1* upon b-induction. (A) Scheme showing the transgenes relevant for the experiment in B as well as the expected cell cycle outcome for each strain. (B) Quantitative RT-PCR for the indicated genes in the different strains. RNA was isolated after 6 h of induction of *nar1* promoter. The expression of *tub1* (encoding Tubulin α) was used as internal control. Values are referred to the expression of each gene in AB34. Each column represents the mean value of four independent biological replicates. Error bars represent mean±s.d.; $^{**}P<0.01$ based on a two-tailed Student's *t*-test to control sample (AB34).

We found that, for all analyzed genes, the levels of mRNA decreased upon b-induced cell cycle arrest. For some genes, like *clb1*, *clb2*, *hsl1* and *plk1*, this decrease was dramatic, whereas for other genes, such as *cdc25* and *wee1*, the decrease was around half the mRNA levels of control conditions (AB34) (Fig. 1B). However, in general, this decrease seems to be a consequence of the cell cycle arrest: interference with the b-induced cell cycle arrest upon expression of the *cdk1*^{AF} allele prevented the decrease in the mRNA levels in all but one case (Fig. 1B). The only exception was observed for *hsl1*, which encodes a putative Nim1-like kinase. In this case, the levels of mRNA decreased upon b-factor expression, regardless of whether cell cycle was arrested or not. Therefore, we considered *hsl1* to be a prime candidate for our study.

Hsl1 kinase is a G2/M cell cycle regulator in *U. maydis*

The Nim1 family of kinases is composed of several serine/threonine kinases that act as negative regulators of Wee1, the mitotic inhibitor

Development (2014) 141, 4817-4826 doi:10.1242/dev.113415

responsible for the Cdk1 inhibitory phosphorylation. In *Saccharomyces cerevisiae*, this family is composed of three kinases, Hsl1, Kcc4 and Gin4 (Barral et al., 1999), whereas in *Schizosaccharomyces pombe*, this family is composed of two members, Nim1/Cdr1 and Cdr2 (Coleman et al., 1993; Feilotter et al., 1991; Kanoh and Russell, 1998; Wu and Russell, 1993). A sequence similarity search of the annotated genome of *U. maydis* indicated that Hsl1 appears to be the single component of this family. A scheme showing the comparison of this predicted *U. maydis* protein with the *S. cerevisiae* and *S. pombe* proteins is presented in Fig. 2A, and the full ClustalW alignment is shown in supplementary material Fig. S1.

To analyze the function of Hsl1, we deleted the *hsl1* gene, replacing it with a hygromycin resistance cassette. The *hsl1* gene is not essential for growth. Mutant cells showed the typical cigar shape as well as a budding pattern similar to wild-type cells (Fig. 2B). The major difference was that mutant cells were more elongated than wild-type cells (Fig. 2B,C). We also found that, for a certain proportion of the population (variable, depending on growth conditions), cell separation was delayed, resulting in cell chains composed of two or three cells (supplementary material Fig. S2; see also Fig. 3A). All these defects were suppressed after the insertion of an ectopic copy of a wild-type *hsl1* gene (supplementary material Fig. S2). In *S. cerevisiae*, Nim1-like kinases were shown to be involved in bud neck morphogenesis, and triple mutants were also affected in cell separation (Barral et al., 1999). We found that in *U. maydis*, an Hsl1-GFP fusion localizes at the bud neck (supplementary material Fig. S3), as it has been described for Nim1-like kinases in *S. cerevisiae*, and which is consistent with a role in cell separation.

The elongated cell phenotype in *U. maydis* has been related to lengthening of the G2 phase (Perez-Martin and Castillo-Lluva, 2008). To test whether this was the case in *hsl1*Δ mutants, we studied the DNA content in cultures of wild-type and *hsl1*Δ mutant strains using FACS analysis. As the length of the different cell cycle phases in *U. maydis* is linked to nutritional conditions (Garrido and Perez-Martin, 2003), we used three different growth media that resulted in distinct FACS profiles. Control cells growing in minimal medium (MMD) showed a prominent peak of G1 cells (1C DNA content), which decreased as the quality of the medium increased (from complete medium/CMD to rich medium/YPD) (Fig. 3A). Interestingly, *hsl1*Δ mutant cells showed the same pattern in all media, consisting of an accumulation of cells carrying 2C DNA content (Fig. 3A). In *S. pombe*, the absence of Cdr2, one of the Nim1-lke kinases, also resulted in a lack of cell cycle adaptation to nutritional conditions, a defect that is exacerbated in the double *nim1* and *cdr2* mutant (Kanoh and Russell, 1998).

Although the accumulation of cells with 2C DNA content in the *hsl1*Δ strain is consistent with an increase of cells in G2 phase, it is worth mentioning that this strain showed cell separation defects. Therefore, a part of the 2C population could be doublets of G1 cells. To circumvent this problem we took advantage of previous studies showing that the mitotic cyclin Clb2 is synthesized during G2 phase and degraded at anaphase, thus providing a reliable marker of G2 phase (Carbo and Perez-Martin, 2010). Wild-type and *hsl1*Δ cells carrying a *clb2-GFP* fusion at its native locus were scored as being in G2 phase or not, based on the presence or absence of a nuclear GFP signal. We observed a dramatic increase in the number of cells showing a Clb2-GFP signal in the *hsl1*Δ mutant strain compared with the wild-type strain (Fig. 3B). Therefore, we conclude that the absence of Hsl1 results in an increase in cells in G2 phase.

Nim1-like kinases are negative regulators of Wee1 kinase in *S. cerevisiae* (McMillan et al., 1999, 2002) as well as in *S. pombe* (Coleman et al., 1993; Wu and Russell, 1993). As Wee1 acts as a mitotic inhibitor, in cells lacking these kinases the G2/M transition is delayed, resulting in a prolongation of G2 phase and, as a consequence, in a cell elongation phenotype. These effects can be suppressed by mutations that disable the Wee1 kinase (Barral et al., 1999; Kanoh and Russell, 1998). We observed that, in a similar way, downregulation of *wee1* expression using a conditional $wee1^{nar1}$ allele (Wee1 is essential in *U. maydis*) suppressed the cell elongation phenotype of *hsl1*Δ cells (Fig. 3C). Also, consistent with a role of *U. maydis* Hsl1 as a Wee1 negative regulator, we found that the levels of Cdk1 inhibitory phosphorylation were higher in *hsl1*Δ cells (Fig. 3D).

In summary, our data show that Hsl1 is a bona fide Nim1-like kinase, acting as a G2/M regulator.

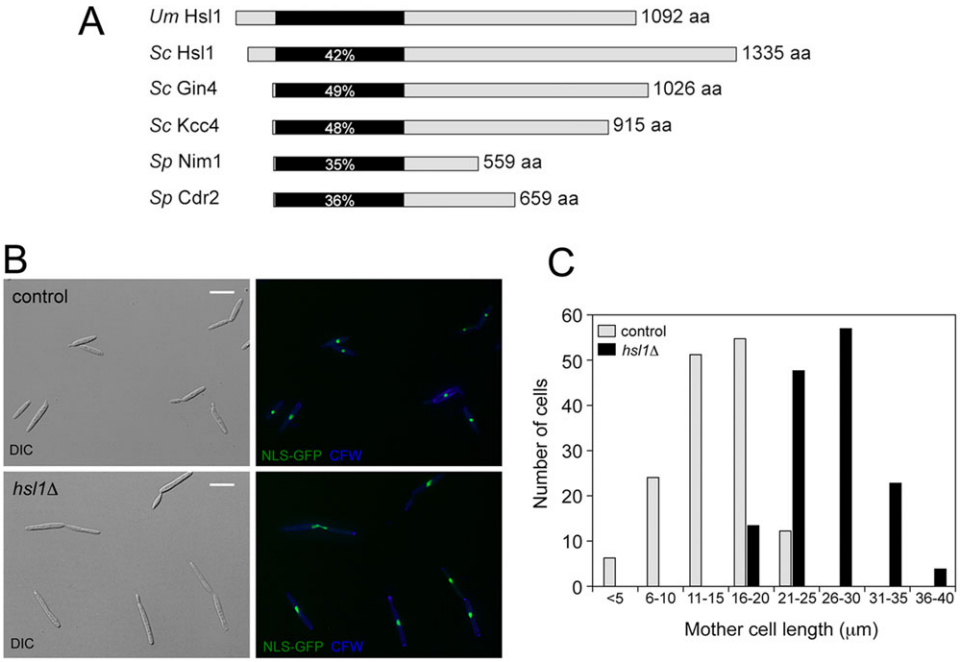

Fig. 2. *hsl1*Δ cells show an elongated morphology. (A) Schematic comparison of the Hsl1 protein with *S. cerevisiae* and *S. pombe* Nim1-like proteins. The catalytic domains are shown in black. The percentages inside each box represent the sequence identity compared with the *U. maydis* sequence. (B) Micrographs showing the cell morphology of control (UMI194) and *hsl1*Δ (UMS60) cells in CMD liquid culture. Cells carried a constitutively expressed NLS-GFP reporter to detect nuclei and were stained with Calcofluor White (CFW) to detect septa. Scale bars: 15 μm. (C) Length of wild-type (FB1) and *hsl1*Δ (MUM1) cells growing in CMD. The length of the major axis of control and *hsl1*Δ mother cells was measured and plotted as a function of the number of cells. A sample of 150 cells was used for each measurement.

Development (2014) 141, 4817-4826 doi:10.1242/dev.113415

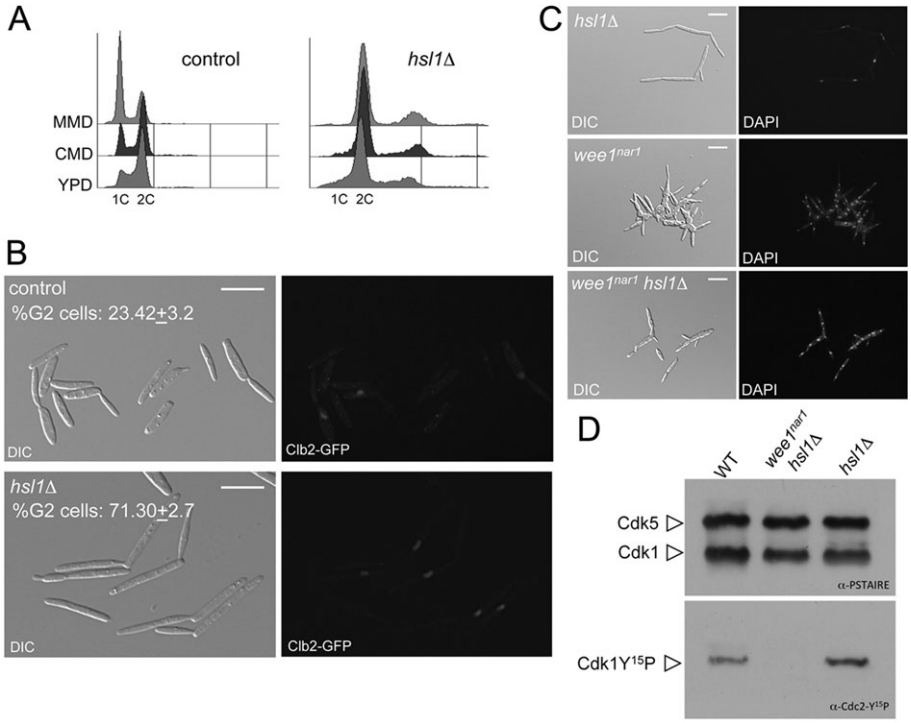

Fig. 3. Hsl1 is a G2/M cell cycle regulator in *U. maydis*. (A) FACS analysis of wild-type (FB1) and *hsl1*Δ (MUM1) cells. Asynchronous cultures of the indicated strains were grown in liquid YPD, CMD or MMD medium. 1C and 2C indicate single and double DNA haploid content. The peak of cells on the right with DNA content higher than 2C is composed of a cell population delayed in cell separation and thereby forming cell chains composed of two or three cells. (B) Cell population showing the G2 marker Clb2-GFP. Control (UMA88) and *hsl1*Δ (UMS59) strains were incubated in CMD. The percentages at the op left corner indicate the percentage of cells in G2 phase as scored for the presence of Clb2-GFP signal (100 cells per experiment, two independent experiments). Scale bars: 20 µm. (C) Epistatic analysis of *hsl1* and *wee1*. The single-mutant *hsl1*Δ (MUM1) and *wee1*^{nar1} (UMC23) as well as the double-mutant *hsl1*Δ *wee1*^{nar1} (UMS61) strains were grown in restrictive conditions for *nar1* expression (YPD) for 8 h. Note that the phenotype of the double mutant in these conditions is similar to the phenotype of the *wee1*^{nar1} cells. Scale bars: 15 µm. (D) Tyrosine phosphorylation of Cdk1 in cells lacking Hsl1. Protein extracts from the strains indicated (FB1: WT; UMS61: *hsl1*Δ *wee1*^{nar1}; MUM1: *hsl1*Δ) were obtained after 8 h of incubation in YPD media. The membrane was probed with anti-phospho-Cdc2 (Tyr15) and anti-PSTAIRE antibodies, which recognize Cdk1 as well as Cdk5, a second CDK from *U. maydis*.

Downregulating expression of *hsl1* and activating Chk1 collaborate in the b-induced cell cycle arrest

The previous results indicated that the downregulation of *hsl1* mRNA levels seems to be an effect of the induction of the transcriptional *b*-program and not a consequence of the cell cycle arrest. In addition, the deletion of *hsl1* in haploid cells growing in axenic conditions produced a G2 cell cycle delay. These results supported our initial hypothesis that additional mechanisms are recruited to sustain a long-term cell cycle arrest during the infective filament formation, and that these mechanisms are most likely related to b-dependent transcriptional changes of regulatory genes needed for G2/M transition. Consequently, we tested whether the downregulation of *hsl1* expression upon *b*-induction was responsible for the observed cell cycle arrest. Our attempts to disable the b-dependent downregulation of *hsl1* by removing transcriptional factors downstream of b factor were unsuccessful (supplementary material Fig. S4). Therefore, we decided to circumvent the downregulation of *hsl1* by exchanging the native *hsl1* promoter with the strong constitutive *tef1* promoter (which renders the *hsl1*^{tef1} allele). We chose this promoter because its activity was refractory to inhibition by the b-dependent transcriptional program (see below), and because it was able to produce transcriptional levels roughly similar to the native *hsl1* promoter in minimal medium (supplementary material Fig. S5).

To address the effect of sustained transcription of *hsl1* mRNA during the induction of the infective filament, we introduced the *hsl1*^{tef1} allele into the UMP112 strain. This strain is derived from AB33 and carries a GFP fusion to a nuclear localization signal under control of the *dik6* promoter. Because the expression of *dik6* promoter is dependent on an active b heterodimer (Brachmann et al., 2001), this strain provides use of the nuclear fluorescence as a visual reporter for the release of cell cycle arrest (counting the nuclear content of the filaments) as well as a surrogate marker of the ability of the different mutants to respond to the b-program. In addition, to analyze the possible joint contribution to cell cycle arrest of *hsl1* downregulation and activation of the DDR pathway, we also combined the *hsl1*^{tef1} allele with the deletion of *chk1*.

First, we observed that, for filaments carrying the *hsl1*^{tef1} allele, the content of *hsl1* mRNA was maintained at a high level upon b-factor induction (Fig. 4A), bypassing the b-dependent transcriptional downregulation described above. Second, we found no difference in the proportion of cells responding to b-factor in the different mutant backgrounds. Even at short times upon induction of *b* expression (4 h), almost the entire cell population showed nuclear fluorescence (supplementary material Fig. S6), indicating that there was no interference with the b-induced transcriptional program. The filaments that constitutively express *hsl1* showed a bulbous structure at the neck of the filament (supplementary material Fig. S6). We have previously reported a similar structure at the neck of filaments produced by cells lacking septins in *U. maydis* (Alvarez-Tabares and Pérez-Martín, 2010), suggesting that the constitutive expression of *hsl1* in the filament could be affecting the septin structure at the filament neck.

Unexpectedly, we found that sustained levels of *hsl1* mRNA alone seem to have no effect on the cell cycle arrest during filament induction. No difference between control (UMP112) filaments or

Development (2014) 141, 4817-4826 doi:10.1242/dev.113415

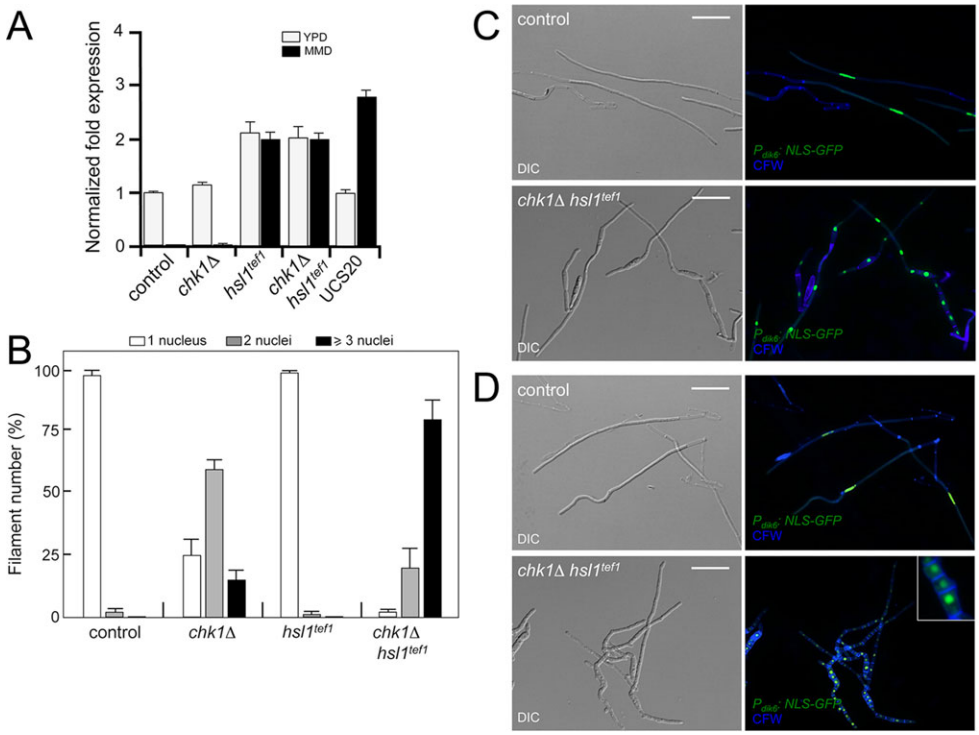

Fig. 4. *hsl1* downregulation and Chk1 activation collaborate in b-induced cell cycle arrest. (A) Bypassing *hsl1* downregulation upon induction of the b-transcriptional program. The *hsl1* promoter was exchanged with the *tef1* promoter, which is not affected by the b-transcriptional program. As a consequence, *hsl1*^{tef1} is expressed in a constitutive manner regardless of whether the b program was active (MMD) or not (YPD). Strains were UMP112 (control), UMP121 (*chk1*Δ), UMS76 (*hsl1*^{tef1}) and UMS120 (*chk1*Δ, *hsl1*^{tef1}). In our transcriptional analysis we also included the strain UCS20 (a derivative of AB34 carrying the P_{dik6}:*NLS-GFP* transgene). The expression of *hsl1* in UMP112 cells (control) grown in YPD was used as a reference to calculate the normalized fold expression. RNA was isolated after 6 h of induction of the *nar1* promoter. Each column represents the mean ratio of three independent biological replicates. Error bars represent mean±s.d.; $^{**}P<0.01$ based on a two-tailed Student's *t*-test to control sample (UMP112). (B) AB33-derived strains carrying the P_{dik6}:*NLS-GFP* transgene and the indicated mutations (control, UMP112; *chk1*Δ, UMP121; *hsl1*^{tef1}, UMS76; *chk1*Δ *hsl1*^{tef1}, UMS120) were incubated in inducing conditions (MMD) for 8 h. Filaments were sorted as carrying one, two or three and more nuclei. Results are shown from two independent experiments, counting more than 100 filaments each. Error bars represent mean±s.d. (C) Cell images of control (UMP112) and a derived strain lacking the *chk1* gene and carrying the *hsl1*^{tef1} allele (UMS120) incubated for 8 h in inducing conditions (MMD). Strains carried an NLS-GFP fusion under control of the b-dependent *dik6* promoter to detect the nucleus. Cultures were stained with CFW to detect septa. Scale bars: 20 µm. (D) as in C, but after 16 h of incubation. Note that filaments in the double mutant were composed of cell compartments carrying one nucleus each and separated by septa (inset). Scale bars: 20 µm.

filaments carrying the *hsl1*^{tef1} allele alone was found regarding nuclear content (Fig. 4B). By contrast, as previously reported (Mielnichuk et al., 2009), in the *chk1* mutant filaments it was possible to observe two and, less frequently, three nuclei, indicating that they were able to divide once, and occasionally even twice, before they arrested their cell cycle. Strikingly, in combination with the absence of Chk1, the presence of the *hsl1*^{tef1} allele precluded the b-dependent permanent cell cycle arrest. In the double-mutant (*chk1*Δ *hsl1*^{tef1}) strain we observed that the filaments carried several nuclei (Fig. 4C,D). Moreover, these nuclei were separated by septa, indicating that the release from cell cycle arrest was complete, resulting in cell division after each cell cycle. As a consequence, the morphology of the mutant filament was different from the control cell cycle-arrested filament; it resembled the growth of a filamentous fungus.

In summary, our results indicate that two individual mechanisms act in concert to specifically establish immediate and sustained arrest upon *b*-induction during the formation of the infective filament in *U. maydis*.

Strains unable to arrest the cell cycle were severely impaired in virulence

To address the consequences of a defective cell cycle arrest during corn infection by *U. maydis*, we constructed compatible haploid strains (i.e. *a1b1* and *a2b2* mating types) carrying the *hsl1*^{tef1} allele, alone or in combination with the *chk1*Δ allele. Mixtures of compatible strains carrying different mutant combinations (WT, *hsl1*^{tef1}, *chk1*Δ and *hsl1*^{tef1} *chk1*Δ) were used to infect 7-day-old maize seedlings by stem injection. Disease symptoms were scored 14 days after infection according to severity (Kamper et al., 2006) (Fig. 5A). We found that infection with strains unable to arrest the cell cycle permanently (*hsl1*^{tef1} *chk1*Δ) resulted in a dramatic loss of virulence (Fig. 5A). The most severe symptoms detectable in plants inoculated with *hsl1*^{tef1} *chk1*Δ crosses were small chlorotic spots (Fig. 5B). Only two plants out of 67 developed further symptoms (in one of them we observed ligula swelling, whereas in the other plant only small tumors on the injected leaf were observed). By contrast, all plants inoculated with wild-type crosses showed tumor formation (Fig. 5A). Strains carrying a *chk1* deletion alone were less efficient in infecting plants and never produced large tumors, as described before (Mielnichuk et al., 2009), whereas the virulence of strains carrying the *hsl1*^{tef1} allele alone was slightly less severe than that of control strains.

In *U. maydis*, virulence and sexual development are intricately interconnected. A prerequisite for generating the infectious stage is the mating of two compatible haploid cells to form, after cell fusion, the infective dikaryotic filament. As the mating process also involves a transient cell cycle arrest (Garcia-Muse et al., 2003), we tested whether the observed dramatic virulence defects in *hsl1*^{tef1}

Development (2014) 141, 4817-4826 doi:10.1242/dev.113415

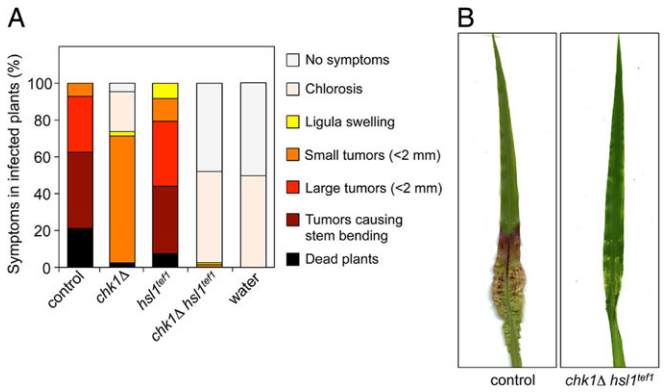

Fig. 5. Inability to arrest the cell cycle results in loss of pathogenicity. (A) Disease symptoms caused by the indicated crosses were scored 14 days after infection of 7-day-old maize seedlings. The *U. maydis* strains used in each cross were FB1×FB2 (control); UMP122×UMP129 (*chk1*Δ); UMS122×UMS124 (*hsl1*^{tef1}); UMS123×UMS125 (*chk1*Δ, *hsl1*^{tef1}) and water as negative control. Symptoms were grouped into color-coded categories depicted on the right side. Two independent experiments were carried out and the average values are expressed as percentage of the total number of infected plants (*n*>50 plants). (B) Photographs of representative leaves 14 days after infection with the indicated *U. maydis* strains.

*chk1*Δ strains were caused simply by the inability to mate. To address this question, we analyzed the presence of b-dependent filaments in crosses of compatible haploid strains on charcoal-containing plates. To distinguish the b-induced filaments from the cell population background (frequently enriched in aberrantly elongated cells) we used haploid strains carrying the P_{dik6}*:NLS-GFP* fusion described above. In this way, only the filaments carrying fluorescent nuclei can be attributed to be the result of a mating process. We observed that wild-type crosses led to white, fuzzy colonies. Microscopic analysis of these colonies showed the formation of b-dependent filaments, which presented two fluorescent nuclei. By contrast, the *hsl1*^{tef1} *chk1*Δ mutant crosses showed an obvious impaired fuzz response. However, we observed filaments with several fluorescent nuclei (Fig. 6A,B), indicating that, although attenuated in filament formation, the *hsl1*^{tef1} *chk1*Δ strains were able to mate.

To test the possibility that the lack of virulence of the *hsl1*^{tef1} *chk1*Δ strain was a consequence of impaired mating, we constructed a double *hsl1*^{tef1} *chk1*Δ mutant in the SG200 genetic background. The SG200 strain is engineered to express both pheromone genes and encodes an active bE1/bW2 heterodimer, which makes it solopathogenic, that is, able to infect plants without mating (Bolker et al., 1995). We infected plants with the SG200 strain as well as with the double *hsl1*^{tef1} *chk1*Δ mutant as described above, and found that the double mutant was entirely unable to infect plants (Fig. 6C), thus ruling out mating deficiency as the reason for the lack of virulence in strains unable to arrest the cell cycle.

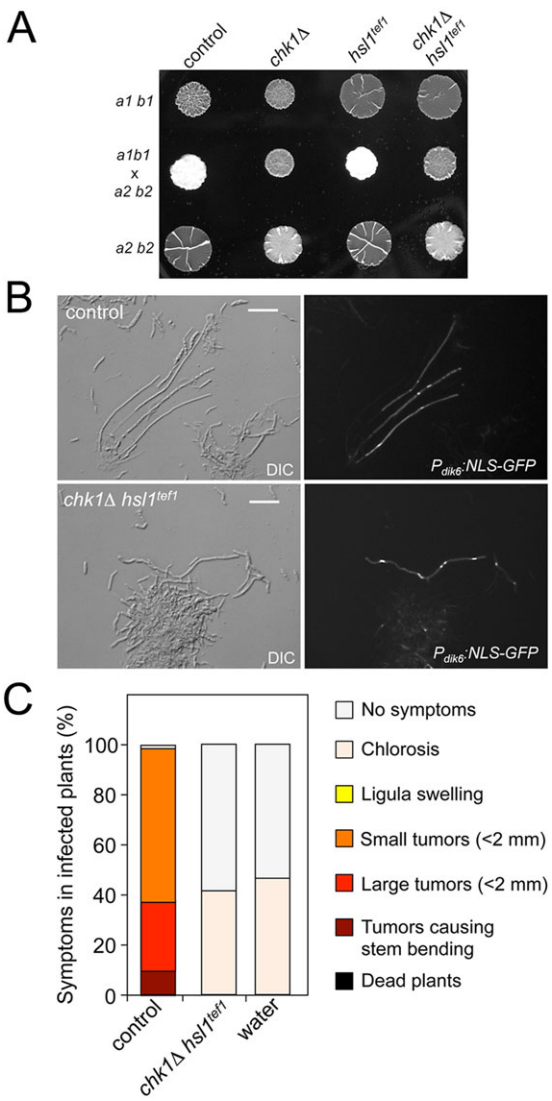

Fig. 6. Lack of pathogenicity is unrelated to mating. (A) Crosses of control as well as single- and double-mutant strains carrying compatible mating types (*a1 b1* and *a2 b2*) in charcoal-containing agar plates The *U. maydis* strains used in each cross were FB1×FB2 (control); UMP122×UMP129 (*chk1*Δ); UMS122×UMS124 (*hsl1*^{tef1}); and UMS123×UMS125 (*chk1*Δ, *hsl1*^{tef1}). (B) Compatible strains carrying an NLS-GFP fusion under control of the b-factor-dependent *dik6* promoter were scraped from the agar surface, mounted on microscopy slides and epifluorescence was observed. Control cross was performed with UMP182 and FB2 strains; *chk1*Δ *hsl1*^{tef1} cross was performed with UMS127 and UMS125 strains. Left panels show differential interference contrast (DIC) microscopy images of cells and right panels show fluorescence in GFP channel. Scale bars: 25 µm. (C) Disease symptoms caused by the solopathogenic SG200 (control) strain and UMS131 (*chk1*Δ, *hsl1*^{tef1}) were scored 14 days after infection. Two independent experiments were carried out and the average values are expressed as percentage of the total number of infected plants (*n*>50 plants).

Cell cycle arrest is required for appressorium formation

To determine the step at which the cell cycle arrest-defective strains were impaired during pathogenic development, we investigated the status of fungal material around the puncture in leaves inoculated with the double mutant cross. We found no evidence of mutant fungal cells inside the plant tissue (supplementary material Fig. S7). A similar experiment performed with wild-type crosses showed fungal hyphae inside the plant tissue (supplementary material Fig. S7). This result suggests that the mutant cells were defective in cuticle penetration and/or subsequent colonization of the plant tissue. The appressorium formation is a requisite for plant penetration, and we therefore decided to search for the presence of appressoria on leaves infected with the double *hsl1*^{tef1} *chk1*Δ mutant. To facilitate the localization of appressoria, we first introduced the AM1 reporter into control (WT) and double mutant combination created in the SG200 genetic background. The AM1 reporter is a transcriptional GFP fusion with the promoter from the gene encoding um01779. This marker shows GFP expression exclusively in those tip cells of filaments that differentiate an appressorium (Mendoza-Mendoza

Development (2014) 141, 4817-4826 doi:10.1242/dev.113415

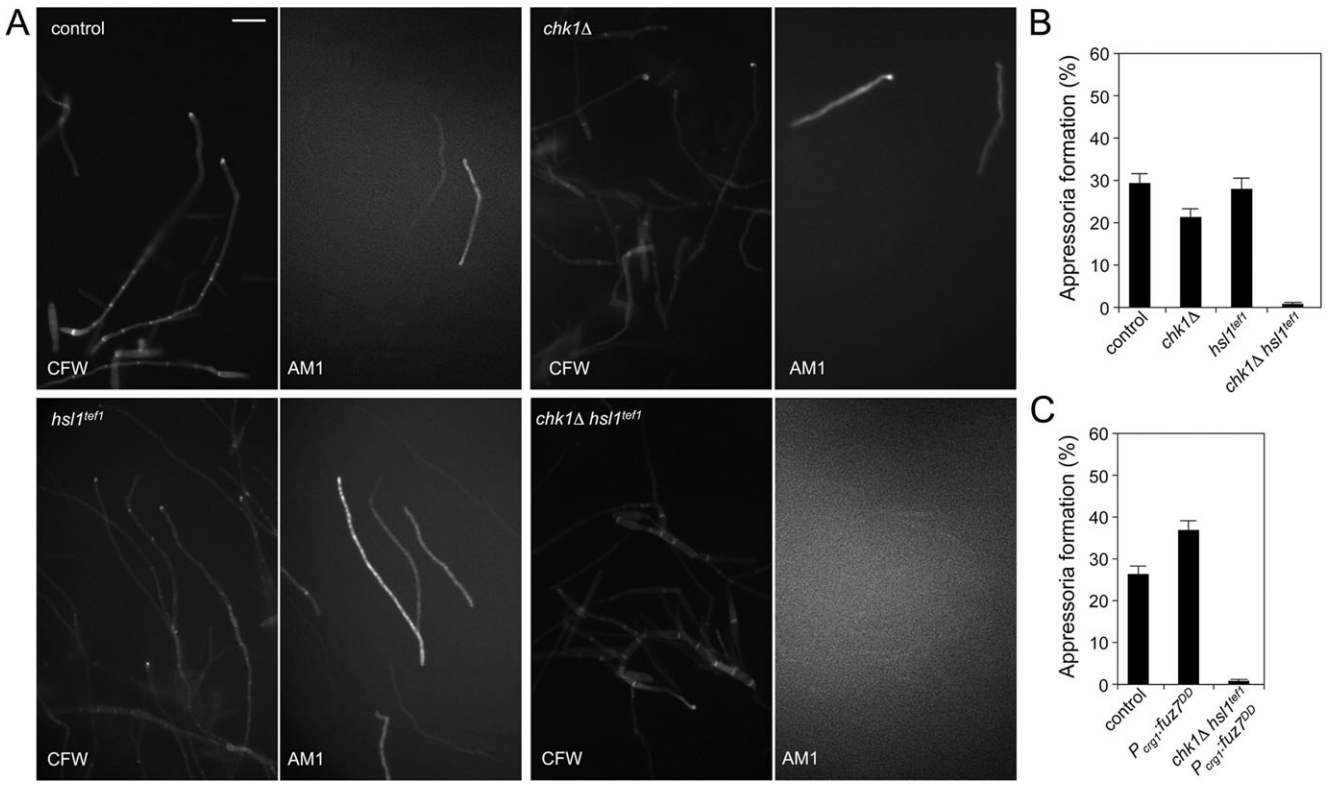

Fig. 7. Appressorium formation requires cell cycle arrest. (A) Appressoria formation on a hydrophobic surface in the presence of hydroxy-fatty acids. Strains used carried the appressorium-specific AM1 reporter as well as the indicated mutations: UMS132 (control); UMS129 (*chk1*Δ); UMS143 (*hsl1*^{tef1}); and UMS137 (*chk1*Δ, *hsl1*^{tef1}). Cells were stained with Calcofluor White (CFW) and analyzed for AM1 marker expression (AM1). Scale bar: 20 µm. (B) Quantification of appressoria formation in the different mutants. (C) Overactivation of the MAPK cascade does not bypass the cell cycle arrest signal. UMS132 (control) as well as the double-mutant derivative (UMS137) were transformed with a construction expressing, under the control of *crg1* promoter, the hyperactivated Fuz7DD MAPKK, resulting in UMS145 (P_{crg1}:*fuz7*^{DD}) and UMS154 (*chk1*Δ, *hsl1*^{tef1} P_{crg1}:*fuz7*^{DD}).

et al., 2009). The leaves were also stained with Calcofluor White (CFW) to detect fungal filaments, as well as to distinguish appressorium formation, which is preceded by formation of a characteristic, crook-like structure that frequently accumulates CFW (Snetselaar and Mims, 1993). By using this approach, we easily found appressoria in wild-type infections, but rarely detected appressoria in the double-mutant strain (supplementary material Fig. S8). We consider this as evidence that, in the absence of a cell cycle arrest, *U. maydis* infective filaments were unable to induce appressorium formation and thereby unable to infect plants.

To provide additional support to this conclusion, we decided to take advantage of previously established *in vitro* conditions to induce appressoria formation in *U. maydis* (Mendoza-Mendoza et al., 2009). We spread wild-type and mutant strains carrying the AM1 reporter on an artificial hydrophobic surface in the presence of long-chain hydroxy fatty acids. After 20 h of incubation, we scored the proportion of filaments (stained with CFW) showing GFP fluorescence (i.e. adopting the appressorium differentiation program). We found that both WT and single mutants were able to produce appressoria at a ratio comparable to those found in other studies for these *in vitro* conditions (Berndt et al., 2010; Freitag et al., 2011; Lanver et al., 2010; Mendoza-Mendoza et al., 2009). In the *hsl1*^{tef1} *chk1*Δ strain, however, we rarely found GFP-positive filaments (Fig. 7A,B).

We were interested in studying which step in the cell cycle arrest affects the ability to produce the appressorium. Activation of the program that produces the appressorium in *U. maydis* involves the sensing of at least two different plant-derived stimuli: a hydrophobic surface and hydroxyl fatty acids. It has been proposed that these signals are sensed, among other elements, by two membrane proteins related to *S. cerevisiae* Sho1p and Msb2p (Lanver et al., 2010), and transmitted by the same MAPK cascade that mediates the pheromone signaling (Mendoza-Mendoza et al., 2009). Mutants lacking these elements, or those unable to process the surface receptors correctly (i.e. showing defects in glycosylation), are severely impaired in their capacity to produce appressoria and subsequently show dramatic defects in virulence (Fernandez-Alvarez et al., 2012; Lanver et al., 2010). Cell cycle regulation could affect the transmission pathway or it could interfere with elements downstream of the signaling cascade. To address whether the cell cycle arrest is affecting the ability to transmit the signal, we introduced into those strains (mutant and WT) that carry the AM1 reporter a construction that expresses the *fuz7*^{DD} allele, encoding a hyperactive version of the pheromone cascade MAPK kinase (Muller et al., 2003) under the control of the *crg1* promoter. We thus bypassed the requirement of the signal transmission upstream of the last step, the activation of the MAP kinase (Kpp2) by its cognate MAPK kinase (Fuz7). We found that even at high levels of activation of the MAPK cascade, the cell cycle arrest was required for appressorium formation (Fig. 7C). These results strongly suggest that the putative targets of the signal emanating from cell cycle arrest are downstream of the MAPK cascade.

DISCUSSION

In response to the activation of the b-dependent transcriptional program, *U. maydis* cells produce an infective filament that is arrested at the G2 stage in the cell cycle. In this study, we found that

Development (2014) 141, 4817-4826 doi:10.1242/dev.113415

hsl1 downregulation upon *b*-induction promotes sustained cell cycle arrest.

Hsl1 belongs to the Nim1 family of kinases. In budding and fission yeasts, these kinases were described as positive regulators of G2/M transition, the inactivation of which resulted in a prolonged G2 phase (Barral et al., 1999; Feilotter et al., 1991; Kanoh and Russell, 1998). We have found a similar effect in *U. maydis* cells lacking Hsl1 during growth in axenic conditions. The cell cycle target of Nim1 kinases in budding and fission yeasts is the kinase Wee1, and our epistasis analysis suggests that it could also be the case for *U. maydis*. In *S. cerevisiae*, the Nim1 family kinases collaborate through a (still unclear) mechanism to promote the degradation of Swe1 (King et al., 2012; McMillan et al., 2002; Sia et al., 1998). By contrast, in *S. pombe*, Nim1 and Cdr2 kinases seem not to affect the protein levels of Wee1 but they inhibit its activity (Coleman et al., 1993; Kanoh and Russell, 1998; Wu and Russell, 1993). We found that, for *U. maydis*, the absence of Hsl1 resulted in an increase in the levels of Cdk1 inhibitory phosphorylation. However, the levels of Wee1 protein in these mutant cells seems to be similar to those observed in control cells (supplementary material Fig. S9). In summary, it is likely that in *U. maydis* Hsl1 assumes some of the roles described in budding and fission yeasts.

Regardless of the actual role of Hsl1 during the vegetative cell cycle in *U. maydis*, here we have examined the relevance of the cell cycle arrest for the infection process. Although sustained *hsl1* expression alone was insufficient to disable the cell cycle arrest upon *b*-induction, we found that, in combination with the deletion of *chk1*, the resulting b-dependent filaments were not cell cycle arrested. The two independent proposed mechanisms seem to act through the same cell cycle regulatory node: the inhibitory phosphorylation of Cdk1. Chk1 activation results in the inhibition of Cdc25, the phosphatase that removes the inhibitory phosphorylation (Mielnichuk et al., 2009; Sgarlata and Perez-Martin, 2005a), whereas in the case of Hsl1 downregulation we suggest that the Wee1 activity – responsible for the inhibitory phosphorylation of Cdk1 – is increased. The imbalance in these opposing activities (phosphatase and kinase) helps to explain the previously observed accumulation of inhibitory phosphorylation in Cdk1 upon activation of the b-dependent transcriptional program, which is ultimately responsible for the cell cycle arrest in G2 (Mielnichuk et al., 2009).

Being able to disable the b-dependent cell cycle arrest, we constructed double-mutant haploid sexually compatible strains, enabling us to address the importance of the cell cycle arrest during the infective process in *U. maydis*. These strains were proficient to mate and to produce infective filaments that were not cell cycle arrested. Importantly, these strains were strongly impaired in their virulence. We found that the mutant infective filaments that did not arrest the cell cycle were unable to produce appressoria, either on the plant surface or on a hydrophobic surface under *in vitro* conditions. The appressorium formation resulted in a localized area of secretion, where plant cell wall-degrading enzymes that help the penetration of the cuticle (Schirawski et al., 2005) and specific effector proteins required for the precise signaling occurring during infection (Djamei and Kahmann, 2012) are concentrated. As a consequence, appressorium formation is essential during the infective process in *U. maydis*, and mutants affected in this step are severely impaired in their virulence (Berndt et al., 2010; Fernandez-Alvarez et al., 2012; Freitag et al., 2011; Lanver et al., 2010). Therefore, it appears that the lack of virulence of non-cell cycle-arrested filaments is a consequence of the inability to produce appressoria.

Basal septation in the b-dependent filament seems to be important for appressorium formation (Freitag et al., 2011). As Hsl1 seems to have some role in septation in *U. maydis*, it is worth noting that the filaments constitutively expressing *hsl1* alone showed no differences in basal septa formation compared with control filaments (supplementary material Fig. S10).

Why does sustaining the G2 cell cycle arrest seem to be important during appressorium formation? In *U. maydis*, as it happens in other systems, entry into mitosis demands the recruitment of a large quantity of cytoskeletal elements to form the mitotic spindle (Straube et al., 2005). On the other hand, the morphogenesis of the appressorium, as well as the support for localized secretion, most likely depend on the coordinated use of both actin- and microtubules-based cytoskeletons, as it has been described for appressorium formation in other fungi (Dagdas et al., 2012). Therefore, it is likely that mitosis and the morphogenetic program responsible for the appressorium formation compete for the same cytoskeletal components. If this is the case, it makes sense that cellular controls exist to force these two processes to be incompatible. Interestingly, this sort of incompatibility is akin to developmental processes in metazoans.

We would like to propose a working model for how the incompatibility between an active cell cycle and appressorium formation is produced (Fig. 8). We considered the notion that the putative regulators that activate the appressorium formation could be downregulated in some way (directly or indirectly) by the activity of the Cdk1-B cyclin complexes. In *U. maydis*, there are two Cdk1-B cyclin complexes (Garcia-Muse et al., 2004). The Cdk1-Clb2 complex is the main activator of mitosis entry and is the target of inhibitory phosphorylation by Wee1 (Sgarlata and Perez-Martin, 2005b). Cdk1-Clb1 in contrast has roles both in G1/S and G2/M transitions (Sgarlata and Perez-Martin, 2005b). We propose that, in order to produce the appressorium, both complexes should be downregulated. According to our model, Cdk1-Clb2 might be repressed through the increase of the inhibitory phosphorylation of the Cdk1 by the two-step mechanism discussed above, whereas the

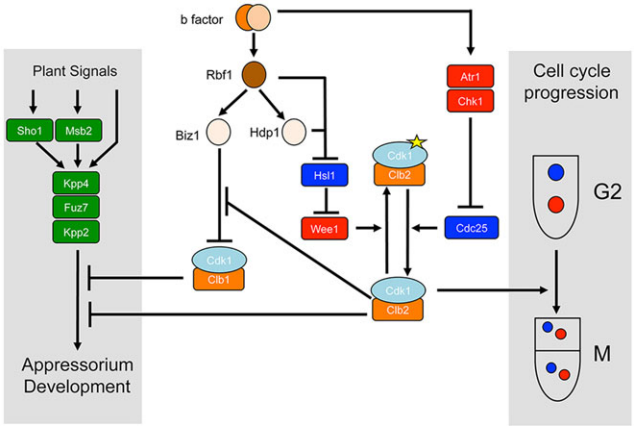

Fig. 8. The developmental program required for appressorium formation is incompatible with an active cell cycle. Cdk1-B cyclin complexes inhibit still unidentified targets required for the formation of appressoria. To allow the induction of appressoria during the infective process, the activity of these CDK complexes should be previously downregulated, which occurs at different levels upon induction of b-factor. Clb1-Cdk1 complexes are downregulated by the action of Biz1, a transcriptional repressor of the *clb1* gene. The Clb2-Cdk1 complexes are repressed by inhibitory phosphorylation of Cdk1 (yellow star), resulting from the upregulation of the kinase Wee1 (because of the b-dependent downregulation of its negative regulator Hsl1) and downregulation of the phosphatase Cdc25 (because of the activation of the DDR kinases Atr1 and Chk1).

Development (2014) 141, 4817-4826 doi:10.1242/dev.113415

Cdk1-Clb1 complex would be repressed through the transcriptional downregulation of *clb1* upon binding of Biz1 to its promoter (Flor-Parra et al., 2006). In both cases, the trigger of these downregulations would be the *b*-factor acting through distinct regulatory circuits. In this study, we have shown that disabling the machinery involved in the inactivation of the Cdk1-Clb2 complex renders the fungus unable to produce appressoria. Furthermore, we previously reported that *U. maydis* cells in which the *clb1* mRNA levels were kept high, because they were either defective in *biz1* or simply bypassing the repression of *clb1* expression by altering the native promoter, were impaired in appressoria formation (Flor-Parra et al., 2006). These two circuits, each devoted to their respective Cdk1-B cyclin complexes, are not independent: we found that the ability of Biz1 to repress *clb1* promoter also requires the prior inhibition of Cdk1-Clb2 complex, as *clb1* expression was not repressed upon ectopic expression of Biz1 in cells unable to phosphorylate Cdk1 at Tyr15 (supplementary material Fig. S11). This additional layer of regulation most likely helps to coordinate the inhibition of both Cdk-B cyclin complexes simultaneously.

In summary, here we provide clues to understand the interdependent relationship between cell cycle regulation and the program devoted to produce appressoria in *U. maydis*. Appressorium formation and cell cycle progression seem to be mutually exclusive choices, a principle that could be applied in a broader sense to other fungal systems.

MATERIALS AND METHODS

Strains and growth conditions

U. maydis strains used were derived from FB1 and FB2 genetic backgrounds (Banuett and Herskowitz, 1989) and are listed in supplementary material Table S1. Cells were grown in rich medium (YPD), complete medium (CMD) or minimal medium (MMD) (Holliday, 1974). Controlled expression of genes under the *crg1* and *nar1* promoters was performed as described previously (Brachmann et al., 2001). FACS analyses were described previously (Garcia-Muse et al., 2003). Details about plasmid and strain constructions, RNA analysis and protein analysis are provided in the supplementary material.

Plant infections, mating assays and appressorium assays

Pathogenic development of wild-type and mutant strains was assayed by plant infections of the maize (*Zea mays*) variety Early Golden Bantam (Olds' Seeds) as described before (Kamper et al., 2006). For mating assays, strains were crossed on charcoal-containing complete medium plates and incubated at 22°C (Holliday, 1974). For appressoria *in vitro* formation, we followed procedures previously described (Mendoza-Mendoza et al., 2009).

Microscopy

Images were obtained using a Nikon Eclipse 90i fluorescence microscope with a Hamamatsu Orca-ER camera driven by Metamorph (Universal Imaging). Images were further processed with Adobe Photoshop CS software.

Acknowledgements

We thank Prof. W. K. Holloman (Cornell University, USA) for proofreading the manuscript. A. Mendoza-Mendoza (Bio-Protection Research Centre, New Zealand) is thanked for advice on *in vitro* appressorium induction. We also thank T. Velasco (CIALE, University of Salamanca, Spain) for greenhouse facilities. Critical reading from Prof. R. Kahmann (MPI, Marburg, Germany) and Prof. G. Steinberg (Exeter University, UK) is also appreciated.

Competing interests

The authors declare no competing financial interests.

Author contributions

N.M. performed the construction of deletion mutant, as well as measurements of Fig. 2B and FACS analysis from Fig. 3A. J.P.-M. constructed the *hsl1*^{tef1} allele. S.C. performed all other experiments. J.P.-M. and S.C. designed the experiments. J.P.-M. wrote the article, with contributions from S.C. and N.M. All authors read, reviewed and approved the final article.

Funding

This work was supported by Grants from the Spanish Government [BIO2011-27773] and EU-Initial Training Network Ariadne [PITN-GA-2009-237936].

Supplementary material

Supplementary material available online at
http://dev.biologists.org/lookup/suppl/doi:10.1242/dev.113415/-/DC1

References

Alvarez-Tabarés, I. and Pérez-Martín, J. (2010). Septins from the phytopathogenic fungus Ustilago maydis are required for proper morphogenesis but dispensable for virulence. *PLoS ONE* **5**, pe12933.

Banuett, F. and Herskowitz, I. (1989). Different a alleles of Ustilago maydis are necessary for maintenance of filamentous growth but not for meiosis. *Proc. Natl. Acad. Sci. USA* **86**, 5878-5882.

Barral, Y., Parra, M., Bidlingmaier, S. and Snyder, M. (1999). Nim1-related kinases coordinate cell cycle progression with the organization of the peripheral cytoskeleton in yeast. *Genes Dev.* **13**, 176-187.

Berndt, P., Lanver, D. and Kahmann, R. (2010). The AGC Ser/Thr kinase Aga1 is essential for appressorium formation and maintenance of the actin cytoskeleton in the smut fungus Ustilago maydis. *Mol. Microbiol.* **78**, 1484-1499.

Bölker, M., Genin, S., Lehmler, C. and Kahmann, R. (1995). Genetic regulation of mating and dimorphism in *Ustilago maydis*. *Can. J. Botany* **73**, 320-325.

Brachmann, A., Weinzierl, G., Kamper, J. and Kahmann, R. (2001). Identification of genes in the bW/bE regulatory cascade in Ustilago maydis. *Mol. Microbiol.* **42**, 1047-1063.

Budirahardja, Y. and Gonczy, P. (2009). Coupling the cell cycle to development. *Development* **136**, 2861-2872.

Carbó, N. and Pérez-Martín, J. (2010). Activation of the cell wall integrity pathway promotes escape from G2 in the fungus Ustilago maydis. *PLoS Genet.* **6**, pe1001009.

Coleman, T. R., Tang, Z. and Dunphy, W. G. (1993). Negative regulation of the wee1 protein kinase by direct action of the nim1/cdr1 mitotic inducer. *Cell* **72**, 919-929.

Dagdas, Y. F., Yoshino, K., Dagdas, G., Ryder, L. S., Bielska, E., Steinberg, G. and Talbot, N. J. (2012). Septin-mediated plant cell invasion by the rice blast fungus, Magnaporthe oryzae. *Science* **336**, 1590-1595.

de Sena-Tomas, C., Fernandez-Alvarez, A., Holloman, W. K. and Perez-Martin, J. (2011). The DNA damage response signaling cascade regulates proliferation of the phytopathogenic fungus Ustilago maydis in planta. *Plant Cell* **23**, 1654-1665.

Djamei, A. and Kahmann, R. (2012). Ustilago maydis: dissecting the molecular interface between pathogen and plant. *PLoS Pathog.* **8**, pe1002955.

Feilotter, H., Nurse, P. and Young, P. G. (1991). Genetic and molecular analysis of cdr1/nim1 in Schizosaccharomyces pombe. *Genetics* **127**, 309-318.

Feldbrügge, M., Kämper, J., Steinberg, G. and Kahmann, R. (2004). Regulation of mating and pathogenic development in Ustilago maydis. *Curr. Opin. Microbiol.* **7**, 666-672.

Fernandez-Alvarez, A., Elias-Villalobos, A. and Ibeas, J. I. (2009). The O-mannosyltransferase PMT4 is essential for normal appressorium formation and penetration in Ustilago maydis. *Plant Cell* **21**, 3397-3412.

Fernández-Álvarez, A., Marín-Menguiano, M., Lanver, D., Jiménez-Martín, A., Elías-Villalobos, A., Pérez-Pulido, A. J., Kahmann, R. and Ibeas, J. I. (2012). Identification of O-mannosylated virulence factors in Ustilago maydis. *PLoS Pathog.* **8**, pe1002563.

Flor-Parra, I., Vranes, M., Kämper, J. and Perez-Martin, J. (2006). Biz1, a zinc finger protein required for plant invasion by Ustilago maydis, regulates the levels of a mitotic cyclin. *Plant Cell* **18**, 2369-2387.

Freitag, J., Lanver, D., Böhmer, C., Schink, K. O., Bölker, M. and Sandrock, B. (2011). Septation of infectious hyphae is critical for appressoria formation and virulence in the smut fungus Ustilago maydis. *PLoS Pathog.* **7**, pe1002044.

Garcia-Muse, T., Steinberg, G. and Perez-Martin, J. (2003). Pheromone-induced G2 arrest in the phytopathogenic fungus Ustilago maydis. *Eukaryot. Cell* **2**, 494-500.

García-Muse, T., Steinberg, G. and Pérez-Martín, J. (2004). Characterization of B-type cyclins in the smut fungus Ustilago maydis: roles in morphogenesis and pathogenicity. *J. Cell Sci.* **117**, 487-506.

Garrido, E. and Pérez-Martín, J. (2003). The *crk1* gene encodes an Ime2-related protein that is required for morphogenesis in the plant pathogen Ustilago maydis. *Mol. Microbiol.* **47**, 729-743.

Heath, I. B. and Heath, M. C. (1979). Structural studies of the development of infection structures of cowpea rust, Uromyces phaseoli var. vignae. II. Vacuoles. *Can. J. Botany* **57**, 1830-1837.

Heimel, K., Scherer, M., Vranes, M., Wahl, R., Pothiratana, C., Schuler, D., Vincon, V., Finkernagel, F., Flor-Parra, I. and Kämper, J. (2010). The

transcription factor Rbf1 is the master regulator for b-mating type controlled pathogenic development in Ustilago maydis. *PLoS Pathog.* **6**, pe1001035.
Holliday, R. (1974). Ustilago maydis. In *Handbook of Genetics* (ed. R. C. King), pp. 575-595. New York: Plenum Press.
Kämper, J., Kahmann, R., Bölker, M., Ma, L.-J., Brefort, T., Saville, B. J., Banuett, F., Kronstad, J. W., Gold, S. E., Müller, O. et al. (2006). Insights from the genome of the biotrophic fungal plant pathogen Ustilago maydis. *Nature* **444**, 97-101.
Kanoh, J. and Russell, P. (1998). The protein kinase Cdr2, related to Nim1/Cdr1 mitotic inducer, regulates the onset of mitosis in fission yeast. *Mol. Biol. Cell* **9**, 3321-3334.
King, K., Jin, M. and Lew, D. (2012). Roles of Hsl1p and Hsl7p in Swe1p degradation: beyond septin tethering. *Eukaryot. Cell* **11**, 1496-1502.
Lanver, D., Mendoza-Mendoza, A., Brachmann, A. and Kahmann, R. (2010). Sho1 and Msb2-related proteins regulate appressorium development in the smut fungus Ustilago maydis. *Plant Cell* **22**, 2085-2101.
McMillan, J. N., Longtine, M. S., Sia, R. A., Theesfeld, C. L., Bardes, E. S., Pringle, J. R. and Lew, D. J. (1999). The morphogenesis checkpoint in Saccharomyces cerevisiae: cell cycle control of Swe1p degradation by Hsl1p and Hsl7p. *Mol. Cell. Biol.* **19**, 6929-6939.
McMillan, J. N., Theesfeld, C. L., Harrison, J. C., Bardes, E. S. G. and Lew, D. J. (2002). Determinants of Swe1p degradation in Saccharomyces cerevisiae. *Mol. Biol. Cell* **13**, 3560-3575.
Mendoza-Mendoza, A., Berndt, P., Djamei, A., Weise, C., Linne, U., Marahiel, M., Vraneš, M., Kämper, J. and Kahmann, R. (2009). Physical-chemical plant-derived signals induce differentiation *in Ustilago maydis*. *Mol. Microbiol.* **71**, 895-911.
Mielnichuk, N., Sgarlata, C. and Perez-Martin, J. (2009). A role for the DNA-damage checkpoint kinase Chk1 in the virulence program of the fungus Ustilago maydis. *J. Cell Sci.* **122**, 4130-4140.
Muller, P., Weinzierl, G., Brachmann, A., Feldbrugge, M. and Kahmann, R. (2003). Mating and pathogenic development of the Smut fungus Ustilago maydis are regulated by one mitogen-activated protein kinase cascade. *Eukaryot. Cell* **2**, 1187-1199.
Pérez-Martín, J. (2009). DNA-damage response in the basidiomycete fungus Ustilago maydis relies in a sole Chk1-like kinase. *DNA Repair (Amst.)* **8**, 720-731.
Perez-Martin, J. (2012). Cell cycle and morphogenesis connections during the formation of the infective filament in Ustilago maydis. In *Morphogenesis and Pathogenicity in Fungi* (ed. J. Perez-Martin and A. di Pietro), pp. 97-114. Berlin; Heidelberg: Springer-Verlag.
Pérez-Martín, J. and Castillo-Lluva, S. (2008). Connections between polar growth and cell cycle arrest during the induction of the virulence program in the phytopathogenic fungus Ustilago maydis. *Plant Signal. Behav.* **3**, 480-481.
Pérez-Martín, J., Castillo-Lluva, S., Sgarlata, C., Flor-Parra, I., Mielnichuk, N., Torreblanca, J. and Carbó, N. (2006). Pathocycles: Ustilago maydis as a model to study the relationships between cell cycle and virulence in pathogenic fungi. *Mol. Genet. Genomics* **276**, 211-229.
Scherer, M., Heimel, K., Starke, V. and Kämper, J. (2006). The Clp1 protein is required for clamp formation and pathogenic development of Ustilago maydis. *Plant Cell* **18**, 2388-2401.
Schirawski, J., Böhnert, H. U., Steinberg, G., Snetselaar, K., Adamikowa, L. and Kahmann, R. (2005). Endoplasmic reticulum glucosidase II is required for pathogenicity of Ustilago maydis. *Plant Cell* **17**, 3532-3543.
Sgarlata, C. and Pérez-Martín, J. (2005a). The Cdc25 phosphatase is essential for the G2/M phase transition in the basidiomycete yeast Ustilago maydis. *Mol. Microbiol.* **58**, 1482-1496.
Sgarlata, C. and Pérez-Martín, J. (2005b). Inhibitory phosphorylation of a mitotic cyclin-dependent kinase regulates the morphogenesis, cell size and virulence of the smut fungus Ustilago maydis. *J. Cell Sci.* **118**, 3607-3622.
Sia, R. A. L., Bardes, E. S. G. and Lew, D. J. (1998). Control of Swe1p degradation by the morphogenesis checkpoint. *EMBO J.* **17**, 6678-6688.
Snetselaar, K. and Mims, C. W. (1993). Infection of maize stigmas by Ustilago maydis: light and electron microscopy. *Phytopathology* **83**, 843-850.
Steinberg, G. and Perez-Martin, J. (2008). *Ustilago maydis*, a new fungal model system for cell biology. *Trends Cell Biol.* **18**, 61-67.
Steinberg, G., Schliwa, M., Lehmler, C., Bolker, M., Kahmann, R. and McIntosh, J. R. (1998). Kinesin from the plant pathogenic fungus Ustilago maydis is involved in vacuole formation and cytoplasmic migration. *J. Cell Sci.* **111**, 2235-2246.
Straube, A., Weber, I. and Steinberg, G. (2005). A novel mechanism of nuclear envelope break-down in a fungus: nuclear migration strips off the envelope. *EMBO J.* **24**, 1674-1685.
Sudbery, P. E. and Gladfelter, A. S. (2008). Pathocycles. *Fung. Genet. Biol.* **45**, 1-5.
Wu, L. and Russell, P. (1993). Nim1 kinase promotes mitosis by inactivating Wee1 tyrosine kinase. *Nature* **363**, 738-741.